13th ewtec 2019 Proceedings of the 13th European Wave and Tidal Energy Conference 1-6 Sept 2019, Naples, Italy

# Small scale optimization of an OWC device

Antonino Viviano, Stefania Naty, Rosaria E. Musumeci, and Enrico Foti

***Abstract*—Waves interacting with an Oscillating Water Column (OWC) device transfer part of their energy to the air, which flows through a turbine. For terminator OWC devices, all the remaining amount of incident wave energy is reflected offshore; wave heights and wave related loads at the front wall depend strongly on the characteristics of air-water interactions inside the pneumatic chamber. Therefore, the device efficiency and stability are strictly related to each other. Both issues must be considered in order to carry out an overall optimization of OWC devices. Here, a small scale physical model of OWC has been adopted. The internal chamber geometry and the front wall can be modified easily to test different configurations of the system. In order to evaluate scaling effects, one of the geometry tested is similar to an OWC tested in a large scale facility. All the tests have been executed with a set of 9 irregular wave conditions. The results of the optimization procedure highlight that the reflection coefficient is highly dependent on the submergence of the front wall. In particular, the optimal conditions are achieved when the ratio between such a submergence and the still water depth is about 1/3. The influence of the width of chamber is significant in the OWC optimization and is related to the wave length corresponding to the peak period of the incident waves.**

***Index Terms*—Oscillating Water Column, physical model, variable geometry, irregular waves.**

## I. Introduction

THIS work is carried out in the context of the physical modeling of a generalized OWC, by means of both large and small scale facilities. The large scale model was tested by [1] at the Large Wave Flume (GWK) of the Coastal Research Centre (FZK) in Hannover, and the results of the experiments carried out under irregular (JONSWAP) wave conditions were analyzed in [2] by considering wave reflection and loadings. Since such a model was approximately 1:5 to 1:9 of full scale, it can be considered reliable and poorly affected by scaling effects. The results of those tests at the GWK was also used as benchmark in the model proposed by [3] for estimating wave pressures at the OWC, under regular and irregular waves.

This paper was submitted to Wave / tidal device development and testing section with ID number 1401. This work has been partly funded by the EU funded project HYDRALAB PLUS (proposal number 654110).

A. Viviano is with the Department of Civil Engineering and Architecture, University of Catania, via S. Sofia 64, 95123 Catania, Italy, and with the Port System Authority of the Western Sicilian Sea, via Piano dell'Ucciardone 4, 90139 Palermo, Italy (e-mail: viviano@portpalermo.it).

S. Naty, is with the Department of Civil Engineering and Architecture, University of Catania, via S. Sofia 64, 95123 Catania, Italy (e-mail: stefanianaty@virgilio.it).

R. E. Musumeci is with the Department of Civil Engineering and Architecture, University of Catania, via S. Sofia 64, 95123 Catania, Italy (e-mail: rmusume@dica.unict.it).

E. Foti is with the Department of Civil Engineering and Architecture, University of Catania, via S. Sofia 64, 95123 Catania, Italy (e-mail: efoti@dica.unict.it).

A crucial aspect in OWC dynamics is the air compressibility, which regulates the intensity and delay of the response of the device to the incident waves, as hilighted in [4] and [5]. Air compressibility is also the main cause of scale effects in physical models. As suggested in [6], different scaling factors should be used for simulating the dynamics of wave and air. This can be obtained by linking the pneumatic chamber with an air tank, as in [7].

The large scale tests at GWK provided a lot of interesting insights for the geometry tested in [1], but they were not designed to allows the variation of the geometry of the device, so they cannot be used for optimization. In order to provide a easy to manage and reliable tool for physical modeling of OWCs, the large scale model has been reproduced at small scale at the Hydraulic Laboratory of the University of Catania (CT), by using a variable geometry system. Viviano et al. [8] evaluated the scale effects of the basic CT model, which reproduces in scale 1:18 the GWK model considering only the height of the chamber, which can be raised in order to limit scaling issues due to air compressibility. They showed that downscaling the OWC causes a reduction of the reflection coefficient and of the extreme wave loads, which are in part recovered by increasing the height of the device.

The physical modeling system proposed by [8] has been adopted here for optimizing the device. In particular, several geometric parameters have been varied. All the tests have been carried out using wave conditions scaled 1:18 with respect to GWK tests.

In the following Section II the new experiments carried out are described, with particular attention to the description of the adopted modeling system with variable geometry. Section III furnishes the main results of the experiments. The conclusions are reported in Section IV.

## II. Description of the Experiments

Wave-air interaction inside the pneumatic chamber of an OWC is a very complex process. The present work adopts the physical modeling approach to optimize the device.

A new laboratory campaign has been carried out, in the same flume adopted for estimating scale effects of a physical model of a generalized OWC [8]. Such effects were analyzed in a model scaled 1:18 of that tested in the large scale at the GWK facility [1].

The flume adopted here is located at the Hydraulic Laboratory of the University of Catania. It is 18 m long, 1.0 m wide and 1.2 m high. As showed in Figure 1, the OWC model is placed on a slope $s = 1 : 6$. Such a model is made of steel and is characterized by a

  

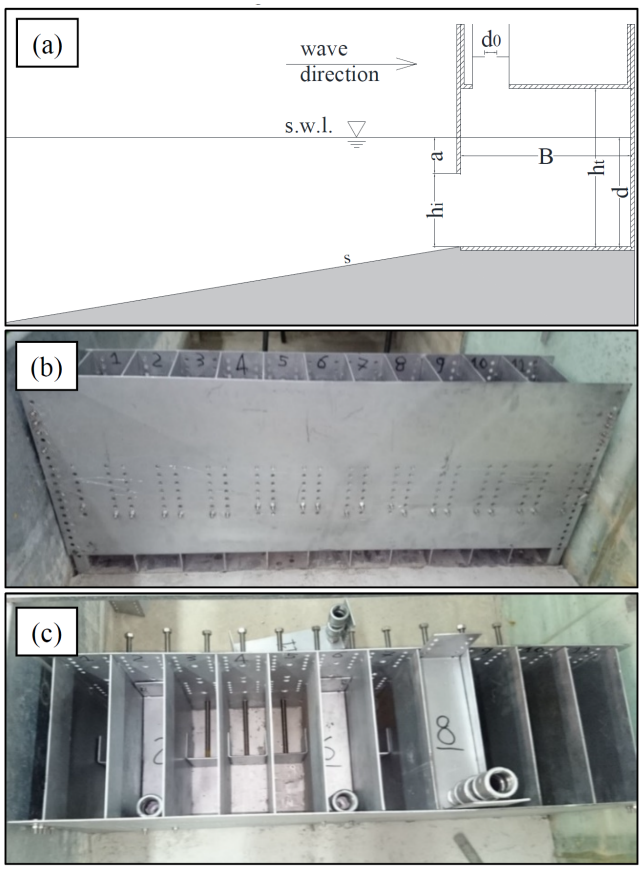


Fig. 1. Physical model of a generalized OWC device, which can vary the submergence of the front wall and the internal chamber height and width: (a) schematic section; (b) front view; (c) upper view.

fixed basis separed in 11 chambers, having the same transverse width $B_t = 0.08m$. The front wall is a sheet which can be mounted on the basis of the model at different heights, so allowing for the variation of the gap height $h_i$ at the front wall.

Each chamber is delimited on the rear part by means of a C-shaped piece welded to a screw, which allows for the variation of the chamber longitudinal width $B$. The variation of the chamber height $h_t$ is obtained by substituting the rear plate, and its screw. The roof of each chamber is constituted by another C-shaped piece on which a duct is mounted with an internal circular restriction (the orifice) having variable diameter $d_0$.

Table II shows a list of the main geometrical parameters of the model. As explained above, four independent parameters are varied, so obtaining 22 different geometrical configurations. The tested configurations do not include the reference model setup, similar to the GWK model [1], i.e. $B = 0.14$ m, $h_i = 0.06$ m (and $a = 0.03$ m), $d_0 = 0.011$ m, $h_t = 0.13$ m. Indeed, such a configuration was already analyzed in a previous paper [8] together with the highest roof condition $h_t = 0.28$ m.

It is worth to point out that the chamber has been sealed at each change of configuration by means of an adequate nautical adhesive tape.

Each geometrical configuration has been tested using irregular mean-JONSWAP incident wave conditions, identical to that used for the scaling effect CT-tests [8],

TABLE I
LIST OF THE GEOMETRICAL PARAMETERS ADOPTED IN THE EXPERIMENTS.

| Geometrical parameter | Tested values |
|---|---|
| $s$ | 1:6 |
| $B$ | 0.05 m ; 0.10 m; 0,14 m |
| $B_t$ | 0.08 m |
| $h$ | 0.19 m |
| $d$ | 0.09 m |
| $a$ | 0.015 m; 0.03 m; 0.05 m |
| $h_i$ | 0.04 m; 0.06 m; 0.075 m |
| $d_0$ | 0.006 m; 0.011 m |
| $h_t$ | 0.13; 0.28 m |

$s$ is the approach slope;
$B$ is the longitudinal width of chamber;
$B_t$ is the transverse width of chamber;
$h$ is the water depth from flume floor;
$d$ is the water depth from the caisson floor
$h_i$ is the height of gap of front vertical wall;
$a$ is the draft of front vertical wall;
$d_0$ is the orifice diameter;
$h_t$ is the height of chamber.

TABLE II
INCIDENT IRREGULAR WAVE CONDITIONS TESTED

| Index | $H_{m0,i}$ [m] | $T_p$ [s] | $H^*$ | $B/L_p$ | $s_w$ |
|---|---|---|---|---|---|
| 1 | 0.02 | 0.9 | 0.11 | 0.13 | 0.016 |
| 2 | 0.03 | 1.2 | 0.16 | 0.09 | 0.013 |
| 3 | 0.02 | 1.5 | 0.11 | 0.07 | 0.006 |
| 4 | 0.02 | 0.7 | 0.11 | 0.19 | 0.026 |
| 5 | 0.03 | 0.7 | 0.16 | 0.19 | 0.039 |
| 6 | 0.03 | 0.9 | 0.16 | 0.13 | 0.024 |
| 7 | 0.04 | 0.9 | 0.21 | 0.13 | 0.032 |
| 8 | 0.05 | 1.2 | 0.26 | 0.09 | 0.022 |
| 9 | 0.06 | 1.4 | 0.32 | 0.08 | 0.020 |

$H_{m0,i}$ is the significant wave height;
$T_p$ is the peak wave period;
$H^* = H_{m0,i}/h$ is the relative wave height;
$B/L_p$ is the relative width of chamber;
$s_w = H_{m0,i}/L_p$ is the wave steepness.

and listed in Table II.

All the experiments have been monitored with a frequency of 1000 Hz by using six wave gauges and three pressure sensors. As sketchd in Figure 2, three wave gauges (WG01-03) have been placed on the horizontal flume zone, at relative distances which allow for the application of the three probe method for wave reflection [9], [10].

Two wage gauges (WG04-05) have been placed in front of the OWC in order to extract information on the wave-device interaction. Furthermore, the last wave gauge (WG06) has been introduced in the central pneumatic chamber (N°6) through the orifice and it registers the water oscillation inside the device. Such a central chamber has been also equipped with a pressure sensor (P03) mounted at the roof of the device, which provides the measurement of the air pressure oscillation in the pneumatic chamber.

Two pressure sensors (P01-02) have been embedded in the front wall of the device for estimating the wave impact on the structure. The bodies of these two sensors have been placed inside a lateral chamber (N°10), in order to have a flat external front wall and a

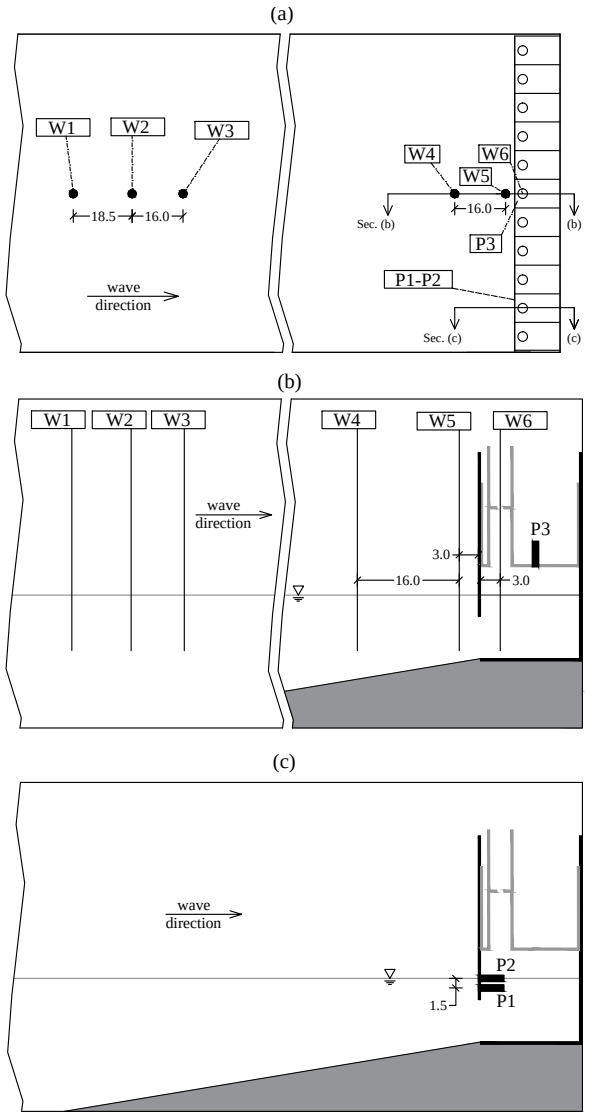


Fig. 2. Sketches of the flume near the device with location of wave gauges W1-W6 and pressure sensors P1-P3: (a) top view; (b) longitudinal section crossing the central chamber where the air pressure and the internal water surface are registered; (c) longitudinal section across the lateral chamber which contains pressures sensors. All the dimensions are expressed in cm.

minimal effect on the remaining measurements, which are instead gathered at the central part of the OWC.

## III. Analysis of the results

The influence on the behavior of the device of the geometrical parameters varied in the experiments (i.e. $B$, $h_t$, $a$, $d_0$) has been analyzed by considering mainly the wave reflection, since it is a phenomenon which is directly related to the efficiency of the device. The pressure distribution has been considered to optimize the device, by comparing it with the basic small scale CT-model similar to the large scale GWK-model.

### *A. Reflection coefficient*

The efficiency of OWC devices has an opposite behavior in comparison to the reflection coefficient $C_r$ [11], which is the ratio between the reflected and the incident significant wave height for irregular waves. Therefore, it is possible to affirm that if is $C_r$ is smaller

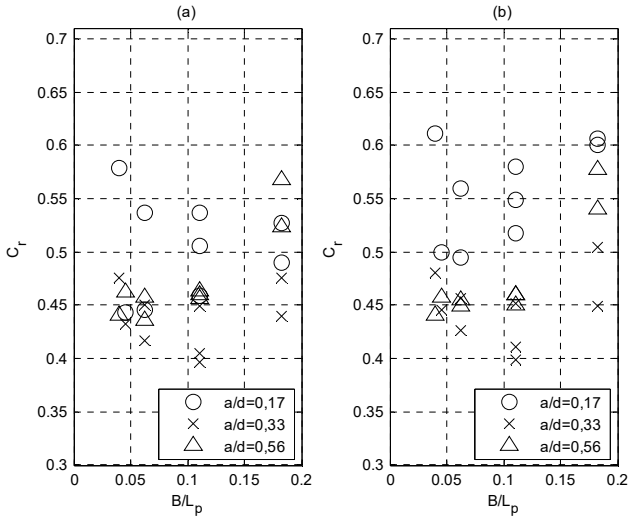


Fig. 3. Reflection coefficent $C_r$ as a function of the ratio $B/L_p$ and $a/d$, for $A_o/A_c = 0.7\%$ ($B = 0.14$ m) and: (a) $h_t/d = 1.44$; (b)) ht/d=3.11.

the amount of wave energy converted by the device and its efficiency are larger.

The optimization of the system is carried out here by considering several dimensionless parameters, which allow to extend the applicability of the obtained results. A first dimensionless parameters is $B/L_p$, which is the ratio between the longitudinal width of the chamber and the wave length calculated by means of the dispersion relationship from the peak wave period $T_p$. The other dimensionless parameters adopted in the efficiency optimization of the device are the relative submergence of the front wall $a/d$, the relative height of the chamber $h_t/d$, and the orifice restriction rate $A_o/A_c$ which is the ratio between the section of the orifice and the horizontal section of the chamber.

Figures 3, 4 and 5 show all the results obtained for fixed $d_0 = 0.011$, which is the $1:18$ geometrical scale value of the GWK tests. What differs in these Figures is the width of chamber $B$, which affects the orifice restriction rate $A_o/A_c$ since the denominator varies. In particular, Figures 3-5 are listed with decreasing $B$ (0.14;0.10;0.05) so they show increasing values of $A_o/A_c$ (0,70%; 0,98% ; 1,96%). In each Figure two subplots are reported with different relative height of the chamber $h_t/d$ which has been varied in order to verify the effect of air compressibility on the results and partially compensate the scale effects due to differences in scaling of air and water. A previous twin study [8] showed that the increase of $h_t$ in small scale model provides always nearest values of $C_r$ to the corresponding large scale model.

Figure 3 and 4 highlight the presence of a minimum of $C_r$ in the range $B/L_p = 0.1 - 0.15$. Figure 5 does not give the same trend since the width $B$ is too low and the values of $B/L_p$ are always lesser than 1. However, the reflection coefficients obtained are the greatest in such a condition ($A_o/A_c = 1.96\%$ and $B = 0.05$ m), it follows that the device is definitely far from its optimum geometry.

The lowest values of $C_r$ (greater efficiency) are ob-

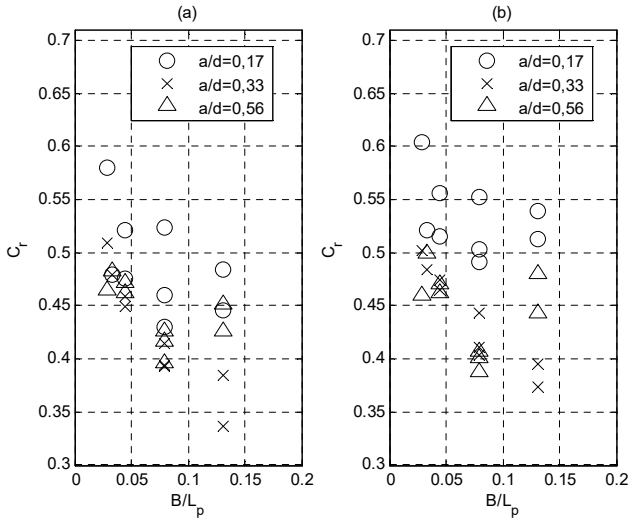


Fig. 4. Reflection coefficent $C_r$ as a function of the ratio $B/L_p$ and $a/d$, for $A_o/A_c = 0.98\%$ ($B = 0.10$ m) and: (a) $ht/d = 1.44$; (b)) ht/d=3.11.

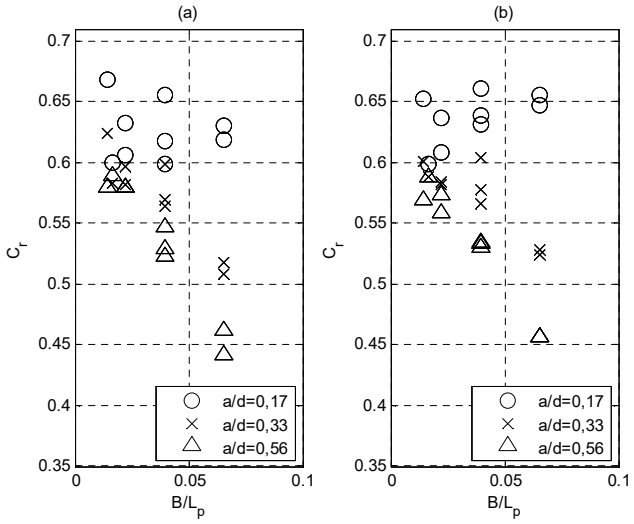


Fig. 5. Reflection coefficent $C_r$ as a function of the ratios $B/L_p$ and $a/d$, for $A_o/A_c = 1.96\%$ ($B = 0.05$ m) and: (a) $ht/d = 1.44$; (b)) ht/d=3.11.

tained for an orifice restriction rate $A_o/A_c = 0.98\%$, i.e. in Figure 4. In such a condition, the minimum reflection coefficient is achieved for a relative draft of the front wall $a/d = 0.33$.

In all tests reported in Figure 4, the increase of chamber height $h_t$ causes a general increases of the reflection coefficient values, but the observed trend is maintained. Therefore, scale effects seems to not have effect on the optimization of the device.

### *B. Pressure distribution*

The analysis of pressure distribution has been focused on the configurations of the device which causes a minimum reflection coefficient, i.e. for the optimized configuration found above having $a/d = 0.33$, $h_t/d = 3.11$ and $A_0/A_c = 0.7$.

The wave condition chosen in this analysis corresponds to index 6 in Table II. It has intermediate

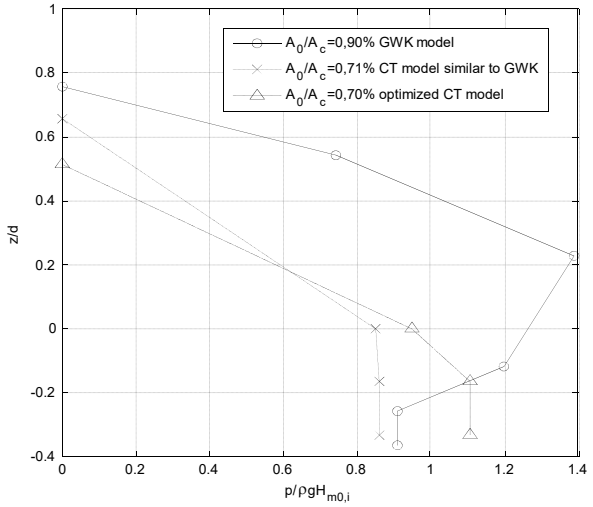


Fig. 6. Dimensionless pressure ($p/\rho gH$) at the front wall for the GWK model(circles), for the CT model similar to GWK (crosses), and for the optimized CT model (triangles).

characteristics among those tested, indeed its steepness is $s_w = 0.024$.

The pressures at the front wall are made dimensionless by dividing them for $\rho g H_{m0,i}$, where $H_{m0,i}$ is the incident wave height. The vertical dimension $z$ is also made dimensionless, by dividing it for the water depth at the device $d$.

Figure 6 shows the dimensionless vertical profile of the pressures induced by waves, in which the optimized configuration found here is compared with the large scale model tested at GWK and with the small scale CT-model similar to the GWK-model, but with the increased height of the chamber.

It is possible to see that the maximum pressure for the large scale model is always greater than the small scale model. Such a scale effect must be considered in the analysis of the results of all the small scale models.

The comparison between the two small scale models shows that the optimized device causes an increase of maximum pressure of about 20%.

## IV. CONCLUSIONS

The optimization procedure of a generalized OWC has been carried out on the basis of physical modeling test. The parameter chosen for easily executing the optimization of the device is the reflection coefficient since it is directly related to wave energy absorbed by the device.

The results of the optimization procedure highlight that the reflection coefficient is highly dependent on the submergence of the front wall. In particular, the optimal conditions are achieved when the ratio between such a submergence and the still water depth ($d$) is about 1/3. The variation of the orifice dimension in a range compatible with the PTO functionality does not show a strong effect on the OWC response. Finally, the influence of the width of chamber ($B$) is significant in the OWC optimization and is related to the wave length corresponding to the peak period of the incident

waves ($Lp$). The optimal values of the ratio $B/Lp$ are obtained in the range $0.1 - 0.15$.

The analysis of the wave related pressures for the optimized device shows an increase of 20% of the maximum pressure near the lip of the front wall, which is the weakest point of the OWC systems.

## ACKNOWLEDGEMENT

This work has been partly funded by the EU funded project HYDRALAB PLUS (proposal number 654110) and by the "Three-year Research Programme 2018-2020" of the Dept. of Civil Engineering and Architecture of the University of Catania.

The authors are grateful to Tom Bruce (University of Edinburgh), William Allsop (HR Wallingford) and Diego Vicinanza (University of Campania "Luigi Vanvitelli") for providing the data of the tests carried out at the GWK.

## REFERENCES

[1] W. Allsop, T. Bruce, J. Alderson, V. Ferrante, V. Russo, D. Vicinanza, and M. Kudella, "Large scale tests on a generalised oscillating water column wave energy converter," in *Proceedings of the HYDRALAB IV Joint User Meeting, Lisbon*, 2014.

[2] A. Viviano, S. Naty, E. Foti, T. Bruce, W. Allsop, and D. Vicinanza, "Large-scale experiments on the behaviour of a generalised oscillating water column under random waves," *Renew. Energy*, vol. 99, pp. 875–887, 2016.

[3] K. A. Pawitan, A. S. Dimakopoulos, D. Vicinanza, W. Allsop, and T. Bruce, "A loading model for an OWC caisson based upon large-scale measurements," *Coastal Engineering*, vol. 145, pp. 1–20, 2019.

[4] A. S. Dimakopoulos, M. J. Cooker, and T. Bruce, "The influence of scale on the air flow and pressure in the modelling of oscillating water column wave energy converters," *International Journal of Marine Energy*, vol. 19, no. Supplement C, pp. 272 – 291, 2017.

[5] A. Viviano, R. E. Musumeci, D. Vicinanza, and E. Foti, "Pressures induced by regular waves on a large scale owc," *Coastal Engineering*, Under review.

[6] W. Sheng, R. Alcorn, and T. Lewis, "Physical modelling of wave energy converters," *Ocean Engineering*, vol. 84, pp. 29 – 36, 2014.

[7] A. F. O. Falcao and J. C. C. Henriques, "Model-prototype similarity of oscillating-water-column wave energy converters," *International Journal of Marine Energy*, vol. 6, pp. 18 – 34, 2014.

[8] A. Viviano, S. Naty, and E. Foti, "Scale effects in physical modelling of a generalized OWC," *Ocean Engineering*, vol. 162, pp. 248–258, 2018.

[9] E. Mansard and E. Funke, "The measurement of incident and reflected spectra using a least squares method," in *Proc. 17th Int. Coastal Engineering Conf., ASCE, New York*, 1980, pp. 154–172.

[10] C. Faraci, P. Scandura, and E. Foti, "Reflection of sea waves by combined caissons," *Journal of Waterway, Port, Coastal, and Ocean Engineering*, vol. 141, no. 2, p. 04014036, 2015.

[11] R.-S. Tseng, R.-H. Wu, and C.-C. Huang, "Model study of a shoreline wave-power system," *Ocean Engineering*, vol. 27, no. 8, pp. 801–821, 2000.